Computational Techniques for Neutronics and Photonics Calculations for Fusion Reactor Blankets and Magnet Shields

M. Abdou and C.W. Maynard

January 1972

UWFDM-3

FUSION TECHNOLOGY INSTITUTE

UNIVERSITY OF WISCONSIN

MADISON WISCONSIN

Computational Techniques for Neutronics and Photonics Calculations for Fusion Reactor Blankets and Magnet Shields

M. Abdou and C.W. Maynard

Fusion Technology Institute
University of Wisconsin
1500 Engineering Drive
Madison, WI 53706

http://fti.neep.wisc.edu

January 1972

UWFDM-3

COMPUTATIONAL TECHNIQUES FOR NEUTRONICS AND PHOTONICS CALCULATIONS FOR FUSION REACTOR BLANKETS AND MAGNET SHIELDS

by

M. Abdou and C.W. Maynard

JANUARY, 1972

FDM 3

University of Wisconsin

Nuclear Engineering Department

TABLE OF CONTENTS

		Page
Preface		i
Introduction		1
A.	Neutron and Photon Transport Calculations	3
	Transport Code	5
	Geometry	5
	Neutron Energy Group Structure	7
	Anisotropic Scattering	12
	Nuclear Data	20
	Multigroup Neutron Cross Sections	21
	Multigroup Photon Cross Sections	21
	Secondary Gamma-Ray Production Cross Sections	27
	Coupled Neutron-Gamma Multigroup Calculations	30
B.	Nuclear Heating Rate Calculations	35
C.	The Neutron-Induced Activity of the Blanket and Shield Materials	46
Bibliography		53

Preface

This report is devoted to a discussion of the theory and computational techniques for carrying out the neutronics and photonics calculations for fusion reactor blankets and magnet shields.

In a previous report, a literature survey of neutronics calculations for fusion reactor blankets has been given. The bibliography at the end of this report has been extended to include the references for that survey for the convenience of the reader.

Introduction

This study is concerned with the neutronics and photonics aspects of fusion reactor blanket design. The areas of investigation will be (i) neutron and photon transport calculations, (ii) energy deposition; and (iii) induced activity.

An accurate yet efficient method is clearly required for predicting neutron and photon transport. The neutron and photon fluxes and currents calculated will be used for calculating reaction rates of interest, e.g. tritium producing reactions, neutron multiplication, and leakage. Energy deposition factors are needed for calculating heat generation rates throughout the vacuum wall, neutron moderating region, and the magnet shield. Calculations of the neutron induced activity require formulation of the activity chains for the materials of interest and an accurate description of all density variations for all coupled nuclides.

In addition to the need for a calculational method, it is certainly of prime importance to compile nuclear data for nuclides of potential value in fusion reactor blankets. Of particular interest are the cross sections for neutron induced reactions, gamma-ray production cross sections from these reactions, and the gamma-ray interaction cross sections. The neutron energy range of interest extends from thermal energies up to 14 MeV--

a much larger energy range than is normally encountered in fission reactors. The nuclear data compiled for this work (which is still far from complete) constitute several large data files, and it has been necessary to develop efficient computer programs for retrieval of data for any particular type of calculation

In this section, a brief description is given of the available, developed, and needed computational techniques to be used in this study. The discussion presented here is arbitrarily organized around individual topics. It should be noted, however, that many aspects of the neutronics and photonics calculations are related to each other and this fact has been of prime consideration in developing consistent and capable computational techniques.

A. Neutron and Photon Transport Calculations

In order to calculate neutron and gamma ray fluxes, one must solve the energy dependent Boltzmann, transport equation. Since no analytical solution for this equation exists, a mathematical technique for approximating the solution must be used. An approximation called the discrete ordinates method is sufficiently accurate and reliable; particularly in problems involving deeply penetrating radiation as in the fusion blanket and magnet shield.

Consider the time independent Boltzmann equation

$$\vec{\Omega}.\nabla\vec{\phi}\ (\vec{r},E,\vec{\Omega}) + \Sigma_t(\vec{r},E)\phi(\vec{r},E,\vec{\Omega}) = S(\vec{r},E,\vec{\Omega}) + \iint dE'd\Omega'\Sigma(\vec{r},E' \rightarrow E,\vec{\Omega}' \rightarrow \vec{\Omega})\phi(\vec{r},E',\vec{\Omega}') \qquad (3\text{-}1)$$

where

$\Sigma_t(\vec{r},E) = \Sigma a(\vec{r},E) + \Sigma_s(\vec{r},E)$ = the total cross-section

$\Sigma(\vec{r},E' \rightarrow E,\vec{\Omega}' \rightarrow \vec{\Omega})$ = the transfer cross-section

$S(\vec{r},E,\vec{\Omega})$ = source term (including the fission and independent sources)

$\phi(\vec{r},E,\vec{\Omega})$ = the angular flux

The integral term (the scattering source) in equation (3-1) is the most difficult and needs to be simplified. For this purpose, we expand the angular flux in spherical harmonics and the transfer cross section in Legendre polynomials.

$$\phi(\vec{r},E,\vec{\Omega}) = \sum_{\ell=0}^{\infty} \sum_{m=-\ell}^{+\ell} f_{\ell,m}(\vec{r},E) P_\ell^m(\vec{\Omega}) \tag{3-2}$$

$$\Sigma(\vec{r},E' \to E,\vec{\Omega}' \to \vec{\Omega}) = \sum_{\ell}' q_\ell(E' \to E) P_\ell(\mu_o) N(\vec{r}) \tag{3-3}$$

where $$\mu_o = \vec{\Omega}.\vec{\Omega}' = \cos\theta \tag{3-4}$$

$\vec{\Omega}'$ and $\vec{\Omega}$ are the neutron directions before and after scattering, respectively. In practice, the sum over ℓ will be cut off at L; it is then necessary to specify L+1 cross sections, σ_ℓ, in order to perform the summation. A semi-quantitative criteria for deciding upon L will be given later in this section.

The essential basis of the discrete ordinates method is that the angular distribution of the neutron flux is evaluated in a number of discrete directions, i.e., the angular variable μ is treated as discrete rather than continuous. It is practical when using the discrete ordinates method to introduce a discrete energy variable, by means of a multigroup approximation, and a discrete space mesh for the spatial coordinates. Consequently, all the independent variables of the time-independent transport equation, namely, space $\vec{r}$, direction $\vec{\Omega}$, and energy E, are treated as discrete. The choice of the energy group structure,

spatial mesh, and direction cosines must be decided on carefully. This will be discussed for the particular problem of fusion blanket.

Transport Code

The ANISN[33] code was obtained and modified[34] and it is now operational on the UNIVAC-1108 computer, EXEC-8, available at the Madison Academic Computing Center.

ANISN solves the one-dimensional Boltzmann transport equation with general anisotropic scattering for slab, cylinderical or spherical geometries by employing the diamond difference solution technique. ANISN has an additional capability; the energy, angle, and spatially dependent flux generated as the solution to the Boltzmann equation may be used to perform a group reduction of the cross sections. Detailed information about ANISN is contained in references 33 and 34.

Geometry

Eventually, a three-dimensional transport or Monte Carlo program may be used to handle all the complications of a full-scale fusion blanket design such as full pipes and diverters, etc. No three dimensional transport code exists. DOT[35] is a two-dimensional discrete ordinates transport code which has most of the features of ANISN. However, using Monte Carlo or two or three-dimensional transport codes carries the penalty of requiring much computer time.

In this stage of fusion reactor design, the view is that steady-state fusion reactors will be either cylinderical or

toroidal in geometry. The cylinder is conceived to have a large height to diameter ratio with large plasma diameters anticipated. The toroidal geometry is expected to have an aspect ratio of around 3 with the major diameter so large that the curvature can be neglected in neutronics calculations. In addition, no detailed designs of diverters, feed pipes, and other necessary access regions have been carried out. In fact, from the neutronics point of view the access regions built into fusion blankets will have the effects of (1) having regions of low nuclide density from which the neutrons can stream out of the system affecting the neutron economy and requiring shields somewhere near the outer ends of the ducts; and (2) increasing parasitic absoprtion of neutrons by neutron collisions in the access regions walls. The two effects will have an important bearing on tritium breeding, and the blanket transport calculations may have to be three-dimensional. Due to the lack of detailed information about access regions at present, two or three-dimensional transport calculations are not justified in terms of the reliability and usefulness of the results obtained compared to the computing machine time consumed. At best, one can now investigate the effect of placing artificial holes in the blanket without knowing either where or what shape the real openings will take to build them.

It is concluded that neutronics and photonics parametric studies can best be done in one-dimensional geometry with allowance

in the blanket design for higher tritium production than necessary for other requirements to take care of the losses that will occur where openings appear in the blanket wall.

The calculations will be essentially model-independent. In other words, a stylized fusion reactor consisting of cylindrical annuli will be used; and the calculation results are considered to be applicable whether the cylinder is the center section of a stabilized mirror or is wrapped into a torus. Furthermore, it is expected that the error in using a slab-geometry approximation for cylinders is small on the basis of the large plasma radii anticipated for steady-state fusion reactors, i.e. $\sim$ 5 meters.

Neutron Energy Group Structure

In multigroup calculations, the neutron (and/or photon) energy range of interest is divided into a finite number, G, of intervals separted by the energies Eg, where g= 1,2,3 ---,G. The order of numbering of these energies is such that g increases, as the energy decreases.

In fusion blankets, the energy range of interest for neutrons extends from thermal energies up to approximately 14 MeV. Consequently, for an accurate multigroup calculation, this wide neutron energy range must be divided into a large number of groups. It is necessary that the energy range for a group be chosen such that the variation of important cross sections within the group is reasonably small. Apart from this, the groups are normally

chosen so that the ratio E_g/E_{g+1} is roughly constant (i.e., at equal lethargy intervals).

One hundred energy groups which have the energy boundaries shown in Table 3-1 were used as a starting point for this work. However, since almost all the materials of potential value in fusion blankets show no strong resonances, the cross sections are fairly smooth over essentially the entire energy range of interest, this number of groups is unnecessary for the calculations of this study. In addition, the limitations of computer memory storage, using such an unnecessarily large number of energy groups, would limit our ability to consider a high degree of anisotropy of the elastic scattering and large order angular quadratures.

Another important consideration is that coupled neutron gamma calculations are very efficient, and it is desireable to use this technique here. In this approach, the gamma energy groups are coupled into the neutron energy groups in a manner to be discussed later. Since the computer memory storage required is roughly proportional to the square of the total number of neutron plus gamma energy groups, a group reduction of the cross sections is necessary.

Some test cases have been run which essentially involved reducing the 100 group, P_8 cross section data sets for nuclides of interest to 52 group sets and then performing 52 group calculations with ANISN/1108 of a standard blanket configuration

Table 3.1 Neutron 100 Energy Group Structure in ev.

Group	Group Limits E(Top)		E(Low)		E(Mid Point)	
1	1.4918	(+7)[a]	1.3499	(+7)	1.4208	(+7)
2	1.3499	(+7)	1.2214	(+7)	1.2856	(+7)
3	1.2214	(+7)	1.1052	(+7)	1.1633	(+7)
4	1.1052	(+7)	1.0000	(+7)	1.0526	(+7)
5	1.0000	(+7)	9.0484	(+6)	9.5242	(+6)
6	9.0484	(+6)	8.1873	(+6)	8.6173	(+6)
7	8.1873	(+6)	7.4082	(+6)	7.7977	(+6)
8	7.4082	(+6)	6.7032	(+6)	7.0557	(+6)
9	6.7032	(+6)	6.0653	(+6)	6.3843	(+6)
10	6.0653	(+6)	5.4881	(+6)	5.7767	(+6)
11	5.4881	(+6)	4.9659	(+6)	5.2270	(+6)
12	4.9659	(+6)	4.4933	(+6)	4.7296	(+6)
13	4.4933	(+6)	4.0657	(+6)	4.2795	(+6)
14	4.0657	(+6)	3.6788	(+6)	3.8722	(+6)
15	3.6788	(+6)	3.3287	(+6)	3.5038	(+6)
16	3.3287	(+6)	3.0119	(+6)	3.1703	(+6)
17	3.0119	(+6)	2.7253	(+6)	2.8686	(+6)
18	2.7253	(+6)	2.4660	(+6)	2.5956	(+6)
19	2.4660	(+6)	2.2313	(+6)	2.3486	(+6)
20	2.2313	(+6)	2.0190	(+6)	2.1251	(+6)
21	2.0190	(+6)	1.8268	(+6)	1.9229	(+6)
22	1.8268	(+6)	1.6530	(+6)	1.7399	(+6)
23	1.6530	(+6)	1.4957	(+6)	1.5743	(+6)
24	1.4957	(+6)	1.3534	(+6)	1.4245	(+6)
25	1.3534	(+6)	1.2246	(+6)	1.2890	(+6)
26	1.2246	(+6)	1.1080	(+6)	1.1663	(+6)
27	1.1080	(+6)	1.0026	(+6)	1.0553	(+6)
28	1.0026	(+6)	9.0718	(+5)	9.5483	(+5)
29	9.0718	(+5)	8.2085	(+5)	8.6401	(+5)
30	8.2085	(+5)	7.4274	(+5)	7.8179	(+5)
31	7.4274	(+5)	6.7206	(+5)	7.0740	(+5)
32	6.7206	(+5)	6.0810	(+5)	6.4008	(+5)
33	6.0810	(+5)	5.5023	(+5)	5.7917	(+5)
34	5.5023	(+5)	4.9787	(+5)	5.2405	(+5)
35	4.9787	(+5)	4.5049	(+5)	4.7418	(+5)
36	4.5049	(+5)	4.0762	(+5)	4.2906	(+5)
37	4.0762	(+5)	3.6883	(+5)	3.8827	(+5)
38	3.6883	(+5)	3.3373	(+5)	3.5128	(+5)
39	3.3373	(+5)	3.0197	(+5)	3.1785	(+5)
40	3.0197	(+5)	2.7324	(+5)	2.8761	(+5)
41	2.7324	(+5)	2.4724	(+5)	2.6024	(+5)
42	2.4724	(+5)	2.2371	(+5)	2.3547	(+5)
43	2.2371	(+5)	2.0242	(+5)	2.1306	(+5)
44	2.0242	(+5)	1.8316	(+5)	1.9279	(+5)
45	1.8316	(+5)	1.6573	(+5)	1.7444	(+5)
46	1.6573	(+5)	1.4996	(+5)	1.5784	(+5)
47	1.4996	(+5)	1.3569	(+5)	1.4282	(+5)
48	1.3569	(+5)	1.2277	(+5)	1.2923	(+5)
49	1.2277	(+5)	1.1109	(+5)	1.1693	(+5)
50	1.1109	(+5)	8.6517	(+4)	9.8803	(+4)

Table 3./ Continued

Group	Group Limits E(Top)		E(Low)		E(Mid Point)	
51	8.6517	(+4)	6.7379	(+4)	7.6948	(+4)
52	6.7379	(+4)	5.2475	(+4)	5.9927	(+4)
53	5.2475	(+4)	4.0868	(+4)	4.6671	(+4)
54	4.0868	(+4)	3.1828	(+4)	3.6348	(+4)
55	3.1828	(+4)	2.4788	(+4)	2.8308	(+4)
56	2.4788	(+4)	1.9305	(+4)	2.2046	(+4)
57	1.9305	(+4)	1.5034	(+4)	1.7169	(+4)
58	1.5034	(+4)	1.1709	(+4)	1.3372	(+4)
59	1.1709	(+4)	9.1188	(+3)	1.0414	(+4)
60	9.1188	(+3)	7.1017	(+3)	8.1103	(+3)
61	7.1017	(+3)	5.5303	(+3)	6.3163	(+3)
62	5.5308	(+3)	4.3074	(+3)	4.9191	(+3)
63	4.3074	(+3)	3.3546	(+3)	3.8310	(+3)
64	3.3546	(+3)	2.6126	(+3)	2.9836	(+3)
65	2.6126	(+3)	2.0347	(+3)	2.3236	(+3)
66	2.0347	(+3)	1.5846	(+3)	1.8096	(+3)
67	1.5846	(+3)	1.2341	(+3)	1.4094	(+3)
68	1.2341	(+3)	9.6112	(+2)	1.0976	(+3)
69	9.6112	(+2)	7.4852	(+2)	8.5482	(+2)
70	7.4852	(+2)	5.8295	(+2)	6.6573	(+2)
71	5.8295	(+2)	4.5733	(+2)	5.1847	(+2)
72	4.5733	(+2)	3.5598	(+2)	4.0379	(+2)
73	3.5598	(+2)	2.7536	(+2)	3.1447	(+2)
74	2.7536	(+2)	2.1445	(+2)	2.4491	(+2)
75	2.1445	(+2)	1.6702	(+2)	1.9074	(+2)
76	1.6702	(+2)	1.3007	(+2)	1.4855	(+2)
77	1.3007	(+2)	1.0130	(+2)	1.1569	(+2)
78	1.0130	(+2)	7.8893	(+1)	9.0097	(+1)
79	7.8893	(+1)	6.1442	(+1)	7.0168	(+1)
80	6.1442	(+1)	4.7851	(+1)	5.4647	(+1)
81	4.7851	(+1)	3.7267	(+1)	4.2559	(+1)
82	3.7267	(+1)	2.9023	(+1)	3.3145	(+1)
83	2.9023	(+1)	2.2603	(+1)	2.5813	(+1)
84	2.2603	(+1)	1.7603	(+1)	2.0103	(+1)
85	1.7603	(+1)	1.3710	(+1)	1.5657	(+1)
86	1.3710	(+1)	1.0677	(+1)	1.2193	(+1)
87	1.0677	(+1)	8.3153	(+0)	9.4962	(+0)
88	8.3153	(+0)	6.4760	(+0)	7.3956	(+0)
89	6.4760	(+0)	5.0435	(+0)	5.7597	(+0)
90	5.0435	(+0)	3.9279	(+0)	4.4857	(+0)
91	3.9279	(+0)	3.0590	(+0)	3.4934	(+0)
92	3.0590	(+0)	2.3824	(+0)	2.7207	(+0)
93	2.3824	(+0)	1.8554	(+0)	2.1189	(+0)
94	1.8554	(+0)	1.4450	(+0)	1.6502	(+0)
95	1.4450	(+0)	1.1254	(+0)	1.2852	(+0)
96	1.1254	(+0)	8.7643	(-1)	1.0009	(+0)
97	8.7643	(-1)	6.8256	(-1)	7.7949	(-1)
98	6.8256	(-1)	5.3158	(-1)	6.0707	(-1)
99	5.3158	(-1)	4.1399	(-1)	4.7279	(-1)
100	4.1399	(-1)	3.2243	(-2)	2.1800	(-1)

[a] (±n) represents ($10^{\pm n}$)

and different spectrum. Comparison with 100 group results has shown that the differences in the calculated blanket parameters (e.g. tritium breeding ratio) is negligible. The technique for collapsing group cross sections and the accuracy of the calculated blanket parameters as a function of energy group structure will be taken up in the proposed studies.

Anisotropic Scattering

Because the neutrons produced by D-T reactions have high energies and the first wall and structural materials of the blanket are of relatively high mass numbers, the anisotropy of the neutron scattering will have important effects on the neutron transport. In addition, the gamma transport is an important consideration in the nuclear design of the blanket, and since Compton scattering has an important angle energy correlation which becomes an angle group correlation it is very important to consider the anisotropy of Compton scattering.

(a) Elastic Scattering

Consider a beam of monoenergetic neutrons scattered elastically by a nucleus represented by a potential V(r). The angular distribution of the scattered neutrons in the center-of-mass system may be expanded in Legendre polynomials as:

$$\sigma(\mu_o) = \sum_{\ell=0}^{\infty} \sigma_\ell P_\ell(\mu_o) \qquad (1)$$

Where μ_o is the cosing of the scattering angle in the center-of-mass system. Each term in the sum corresponds to a definite value of angular momentum ℓ. [53] To see the effect of the various angular momentum components on the scattering, the following argument is presented.

The radial wave equation for a particle of energy E which moves in a central field of force is represented by an equivalent one-dimensional problem if the

potential energy function is written as:

$$V_{eff}(r) = V(r) + \frac{\hbar^2 \ell(\ell+1)}{2mr^2} \qquad (2)$$

The second term on the right hand side is called the centrifugal barrier. V_{eff} decreases with r and is equal to the energy of the incident neutron at the classical turning point R (fig. 3.1). For a given energy, R is larger for waves of higher ℓ. That is the large centrifugal barrier for high ℓ makes it improbable for a particle to be found near the center of force. Thus, the partial cross sections, σ_ℓ, tend to decrease with increasing angular momentum (for a given energy). This point is discussed more qualitatively below.

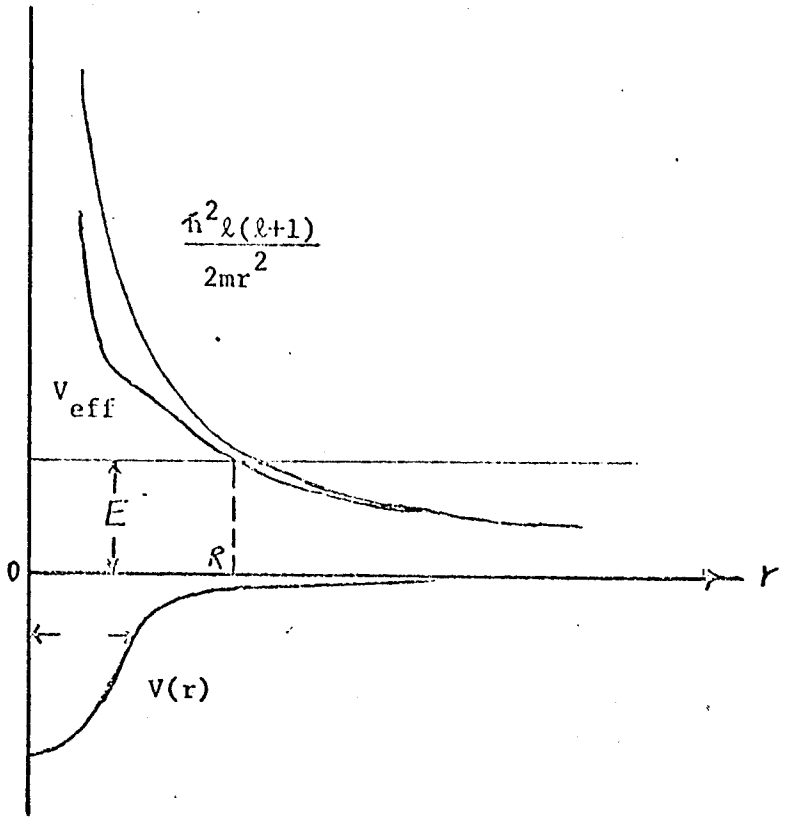

Figure 3.1 The potential function V(r) and $V_{eff}(r)$ for the equivalent one-dimensional problem.

We want to show that the effect of the central force field is negligible for a particle of a given energy E, and sufficiently large ℓ. In figure 3.1, the effective potential is positive to the left of R, and is large near the origin and therefore the radial wave function, U_ℓ, is of exponential type in this region. Near the origin, the wave function is proportional to $r^{\ell+1}$ and therefore it is small in the region in which V(r) is appreciable. To the right of the point R, V(r) is essentially zero and U_ℓ is sinusoidal, behaving exactly like a free particle wave function. Hence, for large r, the effect of V(r) is negligible because it is essentially zero, and for small r the large centrifugal barrier for high ℓ makes the effect of V(r) negligible. Therefore, the intermediate region in the neighborhood of R is the determining factor; if this region is inside the range of V(r) the effect of the force is appreciable. On the other hand, if the region in the neighborhood of R is outside the range of V(r), the effect of the force is small everywhere. In other words, provided that R is greater than a, the range of V(r), the motion of the incident neutron is essentially unaffected by the short range interaction, i.e. no scattering occurs.

The condition that R is greater than a is satisfied if

$$V(R) << \frac{h^2 \ell(\ell+1)}{2mR^2} \tag{3}$$

In this case

$$E = V_{eff} \simeq \frac{h^2 \ell(\ell+1)}{2mR^2} \tag{4}$$

and

$$h^2 \ell(\ell+1) >> 2ma^2 E \tag{5}$$

This is the criterion for σ_ℓ, to be negligible. "a" is the range of V(r) and it is approximately equal to the sum of the nuclear radius and the range of the nuclear forces from the "surface" of the target nucleus, i.e.

$$a \simeq (1.25A^{1/3}+1.0) \times 10^{-13}\text{cm} \tag{6}$$

where A is the nuclear mass number. Condition (5) can be rewritten as

$$\sqrt{\ell(\ell+1)} >> (0.3A^{1/3}+0.24)\sqrt{E} \tag{7}$$

where E is the neutron energy in MeV.

All the refractory metals suggested for use in fusion reactor blankets have mass numbers less than 100. Therefore, for 14.1 MeV neutrons, partial waves which make negligible contributions are the waves satisfying

$$\ell >> 5 \tag{8}$$

The conclusion from the above is that the order of scattering anistropy approximation in the first region of the blanket must be higher than P_5. It should be noted that the above result (8) establishes only the lower limit on the approximation, i.e. if the approximation includes only $\ell < 5$, the solution is very likely to be poor. How high ℓ should be ($\ell >> 5$) is not obtainable from the above discussion. Before discussing how an adequate limit on ℓ can be obtained, anisotropy in the laboratory system is discussed.

The above discussion refers entirely to scattering in the center-of-mass system and it is necessary to transform the differential cross section to the laboratory coordinate system. This can be carried out using the relation[70]:

$$\sigma(0) = \frac{(1+\nu^2+2\nu\cos 0_o)^{\frac{3}{2}}}{|1+\nu\cos 0_o|} \cdot \sigma(0_o) \qquad (9)$$

where 0= scattering angle in the laboratory system,

0_o= scattering angle in the center-of-mass system, and for neutron elastic scattering $\nu = \frac{m_1}{m_2} \simeq \frac{1}{A}$ (10)

where A is the target nucleus mass number.

From (9) it is noted that scattering which is isotropic in the center-of-mass system will become anisotropic in the laboratory system; in particular, it will be peaked in the forward direction. The effect is not significant for heavy nuclei, but for light nuclei it is very important (e.g. even if the scattering of neutrons by hydrogen is isotropic in the center-of-mass system, there is no back scattering of neutrons from hydrogen in the laboratory system). Therefore, scattering anisotropy will be most pronounced in the scattering of fast neutrons from nuclei of all mass numbers and of neutrons of all energies from light nuclei. Considering the suggested design for fusion blankets and magnet shields, it may be concluded, that neutron scattering anisotropy is very important for all regions of the fusion reactor shell.

The difficulty of determining a particular L for truncating the Legendre polynomial expansion of the differential cross section stems from two facts. First, the convergence of the expansion is slow for some elements (e.g. Lithium-7). Second, the error involved in truncating the expansion is not to be measured in terms of the error in estimating the differential cross section but in terms of the effect of the truncated terms on the anisotropy of the angular flux and hence on the desired results. To see this more clearly, consider the scattering source in the transport equation (see Appendix-A) which can be written as

$$\text{scattering source} = \int dE' \int d\vec{\Omega}' \Sigma(r, E' \to E, \vec{\Omega}' \to \vec{\Omega}) \psi(\vec{r}, E', \vec{\Omega}') \qquad (11)$$

The flux can be expanded in associated spherical harmonics and the transfer cross sections in Legendre polynomials as follows:

$$\psi(\underline{r},E,\underline{\Omega}) = \sum_{\ell=0}^{\infty} \sum_{m=-\ell}^{+\ell} f_{\ell_m}(\underline{r},E) P_\ell^m(\underline{\Omega}) \tag{12}$$

and

$$\Sigma(\underline{r},E' \to E,\underline{\Omega}' \to \underline{\Omega}) = \sum_{\ell=0}^{\infty} \Sigma_\ell(\underline{r},E' \to E) P_\ell(\underline{\Omega}.\underline{\Omega}') \tag{13}$$

Making use of the properties of the spherical harmonics, in particular the addition theorem, it can be shown[74] that (11) can be rewritten as

$$\int dE' \sum_{\ell,m} \frac{4\pi}{2\ell+1} \Sigma_\ell(r,E' \to E) f_{\ell,m}(r,E') P_\ell^m(\underline{\Omega}) \tag{14}$$

From this result it is seen that the effect of the ℓth component of the differential cross section, Σ_ℓ, is "weighted" by a corresponding component of the flux. It should be noted that the flux "anisotropy" in a particular region of a system does not depend only on the differential cross section but on characteristics of the whole system. From expression (14) it is noted that the anisotropy of the scattering cross section is important only to the extent that the flux itself is anisotropic and no Σ_ℓ will be significant in the scattering source (and hence in the solution $\psi(\underline{r},E,\underline{\Omega})$ and consequently the desired results) unless the flux also contains an important component of the same order. This observation suggests the following procedure for approximately determining the highest L (in truncating the Legendre expansion of the differential cross section) which has significant contribution to the solution $\psi(\underline{r},E,\underline{\Omega})$. First, the

transport calculation is made with the highest P_L which is practically possible. Second, the angular flux is examined to determine the significant moments. The order of approximation which best fits the angular flux is the order of approximation which should be considered for the differential cross section expansion. Many complicated interrelated factors are involved here. "Computational experiments" will be useful in this regard and further theoretical investigation is needed.

(b) Inelastic Scattering

In compound elastic and inelastic scattering, (n,2n) reactions, and other reactions which pass through the formation of a compound nucleus, the neutrons emitted are often fairly isotropic. However, angular distribution measurements are available for use. Since the anisotropy is not as strong as for elastically emitted neutrons, the order of anisotropy required for elastic scattering angular distributions will be more than adequate for fitting inelastic scattering angular distributions.

(c) Compton Scattering.

The subject of photon collissions and the anisotropy of Compton scattering will be discussed in detail later in this chapter. It may be mentioned here that the applicable differential cross section is a complicated function, and at high energies many terms of Eq. (13) are required to represent the scattering transfer accurately.

(d) Remarks

Adequate representation of anisotropic scattering is extremely important in transport calculations for fusion reactor shells for several

reasons. First, the fusion reactor blanket and shield has a "surface" neutron source at one boundary and the other boundary (shield-magnet boundary) is approximately two meters distant. Thus the fusion reactor shell represents a severe deep penetration problem; the distinguishing characteristic of a penetration problem is that one can not often get by with a poor approximation[32]. Second, the superconducting coils are cryogenically cooled, it is extremely important to calculate the number and energy spectrum of the emerging radiation, and those particles which are scattered with little or no change of direction have the greatest probability of escaping. Therefore, it is particularly important to treat anisotropic scattering accurately. Third, the energy spectrum of neutrons and photons in fusion shells extends to high energies where anisotropy of the scattering is most pronounced.

In addition many considerations have to be taken into account when anisotropic scattering is treated in the discrete ordinates method. For example, angular quadrature sets which correctly integrate Legendre polynomials are required when the problem involves anisotropic scattering. For example, if the flux were constant in angle, the evaluation of the P_2 moment might give a non-zero result, and neutron balance would be affected. In addition, the isotropic component of the flux could include other contributions from higher moments. In general, for anisotropic scattering, the order of the quadrature (n in S_n) should be, roughly, twice as large as L and at least S_4.

NUCLEAR DATA

One of the most important requirements for carrying out the neutronics design of fusion reactor blankets is the availability and accuracy of neutron and photon cross sections for all nuclides used in the blanket over the energy range of interest. One of the goals of this study is to compile a complete set of miscroscopic cross-section data for all nuclides of potential value in fusion reactor blankets. The data should be compiled in a form which can be readily processed by a digital computer.

The philosophy is to obtain fine-group sets based on data which is reasonably well documented and recently evaluated. If some cross-sections have not been measured or if the experimental results are of doubtful accuracy, the cross sections should then be estimated theoretically.

A reliable and efficient way of storing the large quantity of information collected is to employ magnetic tapes using several files. Data retrieval programs have been written to edit, punch, or write on a magnetic tape any required portion of the data. The following subsections are intended as an abstract of the data already obtained and organized in a "Fusion Blanket Neutronics Data Library" hereafter referred to as "FBN/DL". A few words about the sources of data and how it was generated will also be given.

Multigroup Neutron Cross-Sections

Fine-group parameters and group-to-group scattering matrices were obtained as the DLC-2C [39] data package. DLC-2 was generated by the program SUPERTOG [37] from nuclear data in either point-by-point or parametric respresentation forms as specified by ENDF/B [38] version II. This data has been averaged over each specified energy group with the assumption that the flux (used as a weighing function) per unit lethargy is constant. Resolved and unresolved resonance contributions have been calculated where resonance data is available using the infinite dilution approximation. DLC-2 consists of fine group constants such as one dimensional reaction arrays (fission, absorption, etc.,) P_n elastic scattering matrices, and inelastic and (n,2n) scattering matrices which were generated, combined and written in the ANISN format.

The maximum order of approximation to the elastic scattering angular distributions represented in this data is P_8. It has a 100-group structure with energy group boundaries previously shown in Table [3.1]. The data are intended for use in multigroup discrete-ordinates programs (e.g. ANISN) or Monte Carlo transport codes. Information such as inelastic and (n,2n) scattering cross sections can not be obtained from this data since they have already been combined with the elastic scattering matrices.

Multigroup Photon Cross Sections

The gamma cross sections as used in transport and heating calculations result from a simplified picture of the complex

interaction processes of gamma photons with matter. The primary processes that are accounted for in the gamma transport and heating calculations undertaken in this study are the photoelectric effect, Compton scattering, and pair production. All other processes make negligible or very small contributions to the total cross section. The theory of these processes is treated in detail in Heitler's book [51].

The differential scattering law generally used is the formula derived by Klein and Nishina for Compton scattering on the basis of relativistic quantum mechanics. Evans [41] gives an excellent approximation for the differential Klein Nishina collision cross section for unpolarized photons scattered from a free electron at rest as

$$e^{\sigma}(\nu,\theta) = \frac{de^{\sigma}}{d\Omega} = \frac{1}{2} r_o^2 \left(\frac{\nu'}{\nu}\right)^2 \left(\frac{\nu}{\nu'} + \frac{\nu'}{\nu} - \sin^2\theta\right) \qquad (1)$$

and since the frequency of the scattered photon is related to the scattering angle by the relation,

$$\frac{\nu'}{\nu} = \frac{1}{1+\alpha(1-\cos\theta)} \qquad (2)$$

the differential collision cross section can be rewritten as

$$e^{\sigma}(\nu, \theta) = \frac{1}{2} r_o^2 \left[\frac{1}{1+\alpha(1-\cos\theta)}\right]^2 \left\{1+\cos^2\theta + \frac{\alpha^2(1-\cos\theta)^2}{1+\alpha(1-\cos\theta)}\right\} \qquad (3)$$

where

$$r_o = \frac{e^2}{m_o c^2} \text{ (classical electron radius, } 2.818 \times 10^{-13} \text{cm)}$$

e, m_o = are the charge and rest mass of the electron, respectively

ν = frequency of the incident photon

ν' = frequency of the scattered photon

θ = angle between incident and scattered photon directions

$\alpha = h\nu / m_o c^2$

To obtain the expression for the total Compton collision cross section ${}_e\sigma(\nu)$, we integrate Eq.(3) overall permissible values of θ

$$ {}_e\sigma(\nu) = \int_o^{\pi} {}_e\sigma(\nu,\theta) 2\pi \sin\theta d\theta $$

$$ = 2\pi r_o^2 \left[\frac{2(1+\alpha)^2}{\alpha^2(1+2\alpha)} - \frac{1+3\alpha}{(1+2\alpha)^2} - \frac{(\alpha^2-2\alpha-2)}{2\alpha^3} \ln(1+2\alpha) \right] \text{ cm}^2/\text{electron} \quad (4) $$

For photon multigroup calculations, collision cross sections that account for all the photon-electron collisions in a

given energy range comprising a given energy group are needed. The Compton collision cross section for energy group g, ${}_e\sigma^g$, can be obtained by averaging ${}_e\sigma(\nu)$ over the frequency range of group g using the incident photon flux, $\phi(\nu)$, as the weighing function.

$$ {}_e\sigma^g = \frac{\int_{\nu_1^g}^{\nu_2^g} \phi(\nu)\, {}_e\sigma(\nu)\, d\nu}{\int_{\nu_1^g}^{\nu_2^g} \phi(\nu)\, d\nu} \qquad (5\text{-a}) $$

$$ {}_e\sigma^g = \frac{\pi r_o^2 \left(\frac{m_o c^2}{h}\right) \int_{\alpha_1}^{\alpha_2} \left[\frac{2(\alpha^3+9\alpha^2+8\alpha+2)}{\alpha^2(1+2\alpha)^2} + \frac{(\alpha^2-2\alpha-2)}{\alpha^3} \ln(1+2\alpha)\right] \phi(\alpha)\, d\alpha}{\int_{\nu_1}^{\nu_2} \phi(\nu)\, d\nu} \qquad (5\text{-b}) $$

where $$\alpha_1 = \frac{h\nu_1^g}{m_o c^2}$$

$$\alpha_2 = \frac{h\,\nu_2^g}{m_o c^2}$$

and ν_1^g and ν_2^g are the limits of the frequency band.

Since only the energy fraction $h\nu'/h\nu$ appears as scattered radiation, the differential scattering cross section ${}_e\sigma_s(\nu, \theta)$ and the differential collision cross-section have the simple relationship

$$ {}_e\sigma_s(\nu,\theta) = \frac{\nu'}{\nu}\, {}_e\sigma(\nu,\theta) \tag{6} $$

$$ = \frac{r_o^2}{2}\left(\frac{\nu'}{\nu}\right)^3\left(\frac{\nu}{\nu'} + \frac{\nu'}{\nu} - \sin^2\theta\right) $$

or

$$ {}_e\sigma_s(\nu,\theta) = \frac{1}{2}r_o^2\left[\frac{1}{1+\alpha(1-\cos\theta)}\right]^3\left\{1+\cos^2\theta + \frac{\alpha^2(1-\cos\theta)^2}{1+\alpha(1-\cos\theta)}\right\} \tag{7} $$

The scattering cross section, ${}_e\sigma_s$, can be obtained by integrating Eg.(7) over all permissible angles θ. The Compton absorption cross-section, $({}_e\sigma_a)$, is the difference between ${}_e\sigma$ and ${}_e\sigma_s$. The Compton absorption cross section is used in calculating energy deposition from secondary gammas.

To derive the scattering moments of the group transfer cross sections, it is assumed that the Klein-Nishina formula can be represented by

$$\sigma_s^{(i)}(E,0) = \sum_{n=o}^{\infty} \frac{2\ell+1}{4\pi} P_\ell(\cos 0)\sigma_{s\ell}^{(i)}(E \to E') \tag{8}$$

where $\sigma_s^{(i)}(E,0) = {}_e\sigma_s^i(E,0)Z_i$

and Z_i = the atomic number of element i

Using expression (7) for ${}_e\sigma_s^{(i)}$, an expression for $\sigma_{s_\ell}^{(i)}(E,E')$ can be derived from Eq. (8). The required group transfer cross sections for each order of anisotropy, ℓ, are given by

$$\sigma_{s\ell}^{(i)g \leftarrow h} = \frac{\int_{E_{h+1}}^{E_h} \phi(E)dE \int_{E_{g+1}}^{E_g} \sigma_{s\ell}^{(i)}(E \to E')dE'}{\int_{E_{h+1}}^{E_h} \phi(E')dE'} \tag{9}$$

where E_h, E_{h+1} are the energy bounds for the energy group from which the photon is scattered,

and E_g, E_{g+1} are the energy bounds for the energy group to which the photon is scattered.

Almost all existing Computer codes (ref. 43, 44, 45, 48) which generate photon-multigroup cross sections utilize the method outlined above for calculations of gorup transfer cross sections and the contribution of Compton effect to the total collision cross sections. The pair production and photoelectric absorption cross sections are usually read in from a data

library. For example, the computer program GAMLEG 69 uses the analytic approximations presented by Biggs and Lighthill[46],[47].

MUG[48], a revision of program GAMMA, was obtained and operated on the UNIVAC-1108 computer for the purpose of generating photon multigroup cross sections for use in photon transport calculations for the blanket and magnet shield of a fusion reactor. MUG calculates multigroup photon cross sections up to a maximum of 100 groups, with transfer coefficients represented by a Legendre expansion containing terms up to the P_{12} term.

The multigroup photon cross sections generated for this work have a 21-group structure, with the energy group boundaries shown on table 3.2.

Secondary Gamma-Ray Production Cross Sections

In performing gamma-ray transport calculations, secondary gamma-ray spectra must be available in addition to α-group to group cross sections. In the following, the α-ray spectra data used and the code which converts this spectra to secondary gamma-ray production cross sections is discussed.

The availability of the spectra of gamma rays following various neutron induced reactions ((n,γ), $(n,n'\gamma)$, etc.)has increased during the last few years. Yield arrays for reactions are found in the literature in several forms:as the intensity of photons emitted per photon-producing reaction, as the actual cross sections for the production of photons due to the reaction of interest, etc.

The POPOP4 library[52] is a compendium of secondary gamma ray data for the various neutron induced reactions. There are two types of data in the POPOP4 library [52]is a compendium of secondary gamma-ray data for the various neutron-induced reactions. There are two types of data in the POPOP4 library: (1) the intensities of secondary gamma rays resulting from

Table 3.2 Gamma-Ray Energy Group Structure

Group	Energy Limits (Mev)	Mid-Point Energy or Important Line (Mev)
1	14.0 - 12.0	13.0
2	12.0 - 10.0	11.0
3	10.0 - 8.0	9.0
4	8.0 - 7.5	7.75
5	7.5 - 7.0	7.25
6	7.0 - 6.5	6.75
7	6.5 - 6.0	6.25
8	6.0 - 5.5	5.75
9	5.5 - 5.0	5.25
10	5.0 - 4.5	4.75
11	4.5 - 4.0	4.25
12	4.0 - 3.5	3.75
13	3.5 - 3.0	3.25
14	3.0 - 2.5	2.75
15	2.5 - 2.0	2.22[a]
16	2.0 - 1.5	1.75
17	1.5 - 1.0	1.25
18	1.0 - 0.4	0.70
19	0.4 - 0.2	0.30
20	0.2 - 0.1	0.15
21	0.1 - 0.01	0.055

[a]The 2.23 Mev hydrogen capture gamma ray dominates this group.

neutron-nucleus interactions (yields), (2) the secondary gamma-ray production cross sections for neutron-nucleus interactions. The library in its present form contains 243 data sets and a good effort is made to continuously up date it. The POPOP4 library is used with the POPOP4[49] code which generates neutron to gamma-ray multigroup transfer cross sections for eventual use in coupled multigroup calculations. POPOP4 converts the appropriate data sets from the given energy structure to the neutron-gamma multigroup energy structure required for coupled transport calculattions. If a data set is in terms of gamma ray intensities per neutron induced reaction (yields), the code multiplies the converted multigroup intensities by input multigroup neutron reaction cross sections to give multigroup secondary gamma ray production cross sections. The multigroup neutron reaction cross sections must be independently calculated and flux weighted with another appropriate code. ANISN is used for this purpose here. If a data set is given in terms of secondary gamma-ray production cross sections, the code converts the data from a given neutron-gamma energy group structure to the required neutron-gamma energy group structure. Finally, the code sums the converted cross sections for the various reactions included in the calculations, e.g., (n,γ), $(n,n'\gamma)$, etc., to give secondary gamma-ray production cross sections for the nuclide of interest.

It should be noted that the secondary gamma rays produced in calculations using cross sections obtained as described above are assumed to be emitted isotropically. The possibility of incorporating anisotropic production into this procedure will be investigated.

Coupled Neutron-Gamma Multigroup Calculations

For gamma transport calculations, the source of gamma-rays within the blanket must be described accurately. Description of this source requires the calculation of the number, spatial distribution, and energy of secondary gamma-rays produced by neutron-induced reactions within the blanket materials.

One of the possibilities for doing such calculations is to proceed as follows: (i) neutron multigroup transport calculations are performed, (ii) the neutron spatial distribution is then used with the secondary gamma-ray production cross sections for calculation of the gamma-ray source, (iii) this source is used for a second run of the transport code to perform gamma multigroup transport calculations.

Another and more efficient method is to couple the neutron and gamma multigroup cross sections into one multigroup set which can be used for a coupled neutron-gamma multigroup calculation.

To simplify the discussion, consider the Boltzmann transport equation for one of the gamma energy groups, g, with isotropic scattering assumed

$$\vec{\Omega}\cdot\nabla\phi_g(\vec{r},\vec{\Omega}) + \sum_{tr}^{g}\phi_g(\vec{r},\vec{\Omega}) + \frac{1}{4\pi}\phi_g(\vec{r})\Sigma_{sg}(\vec{r})\bar{\mu}_g(r)$$

$$= S_g(\vec{r},\vec{\Omega}) + \frac{1}{4\pi}\sum_{g'}\phi_{g'}(\vec{r})\Sigma_{g'\to g}(\vec{r}) \qquad (1)$$

The terms on the left hand side represent the losses from group g. The second term on the right hand side is the source for group g from downscatter from all higher gamma energy groups. The term $S_g(\vec{r},\vec{\Omega})$ accounts for all gamma production in group g. In the absence of an external gamma-ray source,

the term $S_g(\vec{r},\vec{\Omega})$ is the number of photons produced in group g form all neutron-induced, γ-ray producing reactions for all neutron energies, i.e.

$$S_g(\vec{r},\vec{\Omega}) = N\int\sum_j \phi_j(\vec{r},\Omega')\ \sigma^P_{j\to g}(\vec{\Omega}',\vec{\Omega})\ d\Omega' \qquad (2)$$

where $\phi_j(\vec{r},\vec{\Omega})$ = angular flux for neutron group j

$\sigma^P_{j\to g}$ = number of photons produced with energies in group g from all neutron-induced reactions in neutron group j.

N = nuclide density

In the first method, based on independent neutron and gamma transport calculations, the ϕ_j^S are calculated in the neutron transport run and then used to calculate the S_g^S which are used as an external source input to the gamma calculations.

Next, suppose the neutron cross sections are available for ING neutron groups, the gamma-ray cross sections for IGG gamma groups, and the σ^P cross sections for both the ING neutron and the IGG gamma groups. Let these sets be formed into a cross section set of ING plus IGG groups with the highest neutron energy group as group 1 and the highest gamma energy group as group ING + 1. The transport calculations with the coupled set will not change the neutron calculation procedure, but the transport equation solved for gamma rays will have the secondary gamma-ray source provided for automatically via downscattering terms from neutron energy groups.

A computer code is being written for coupling P_n neutron cross section sets, P_n gamma ray cross section sets, and multigroup secondary gamma-ray production cross sections. To understand the coupling technique explained above and what the coupling code will do, the following discussion is in order.

The coupling program will be written with the output intended for use with the ANISN code. The cross section format required for ANISN is explained in reference[33]. When there is no upscatter and no activity cross sections, ANISN requires a table of cross sections for each energy group g for each material, in the following format:

Position	Cross Section Type
1	σ_a
2	$\nu\sigma_f$
3	σ_T
IHS=4	$\sigma_{g\to g}$
IHS+1	$\sigma_{g-1\to g}$
⋮	⋮
IHM	$\sigma_{g-NDS\to g}$

where IHM is the length of the cross section table, IHS is the position of σ_{gg} (self-scatter) in the cross section table (= 4 when there is no activity cross sections and there is no upscatter), and NDS is the number of groups of downscatter.

Assume that the coupled neutron gamma energy group structure consists of 52 neutron energy groups, and 21 gamma energy groups. Consider a P_o cross

section set. The cross sections for the first 52 groups contain the appropriate σ_a, $\nu\sigma_f$, σ_T, P_o neutron downscatter matrix and zeroes to complete the downscatter matrix. Groups 53 through 73 contain the appropriate σ_{abs}, ($\nu\sigma_f$=0), σ_T, P_o gamma-ray downscatter matrix, and the multigroup secondary gamma ray production cross sections. That is, the positions within the down scatter matrices for groups 52 through 73 -- which represent downscatter from group 1 through group 52 contain the multigroup production cross sections (POPOP4 cross section). As an example, the P_o cross sections for groups 25 and 71 have the following format

Position	Group 25	Group 71
1	σ_a	σ_{abs}
2	$\nu\sigma_f$	0.0
3	σ_T	σ_T
4	$\sigma_{25\to25}$	$\sigma_{71\to71}$
5	$\sigma_{24\to25}$	$\sigma_{70\to71}$
|	|	|
|	|	|
|	|	|
20	$\sigma_{9\to25}$	$\sigma_{55\to71}$
21	$\sigma_{8\to25}$	$\sigma_{54\to71}$
22	$\sigma_{7\to25}$	$\sigma_{53\to71}$
23	$\sigma_{6\to25}$	$\sigma^{P}_{52\to71}$
24	$\sigma_{5\to25}$	$\sigma^{P}_{51\to71}$
|	|	|
|	|	|

Position	Group 25	Group 71
28	$\sigma_{1\rightarrow 25}$	$\sigma^{P}_{47\rightarrow 71}$
29	0.0	$\sigma^{P}_{46\rightarrow 71}$
30	0.0	$\sigma^{P}_{45\rightarrow 71}$
|	|	|
|	|	|
73	0.0	$\sigma^{P}_{2\rightarrow 71}$
74	0.0	$\sigma^{P}_{1\rightarrow 71}$
75	0.0	0.0
76	0.0	0.0

where $\sigma^{P}_{i\rightarrow j}$ is the production cross section from (neutron) group i to (gamma) group j.

The $Pn's^{3}$ for other values of "n" for neutron and gamma-ray cross section sets are similarly coupled.

B) Nuclear Heating Rate Calculations

The engineering design of thermonuclear blankets is largely dictated by the temperature and stress limitations on materials and the methods of heat removal. The heating in the blanket arises from two independent heat loads: (1) the heating by absorption of plasma radiation, and (2) the nuclear heating arising from neutron-induced reactions and secondary gammas. The penetration depth of bremsstrahlung and synchrotron plasma radiation within the first wall (heavy solid) is very small (about 1mm); therefore the energy deposition of the plasma radiation is very nearly a plane source at the vacuum boundary. The amount of heat deposition from plasma radiation will depend on plasma conditions which can not be well defined at the present for a full scale reactor.

The following procedure for heating rate calculations will be adopted. The heat generation ratefrom neutrons and secondary gammas will be investigated in detail. The plasma radiation will be approximately calculated for different sets of plasma conditions; and for each case the plasma radiation heat deposition will be added to the neutron and gamma heat load in the first millimeter of the first wall.

Before going into details about heating rate calculations, it is appropriate to define first the terminology "fluence-to-kerma factors" recommended by the International Commission on Radiological units and Measurements (ICRU)[65] which will be used in this study. In the phrase "Fluence-to-kerma factor", "fluence" is the time integrated flux and "kerma" is the kinetic energy released in materials. Kerma is defined as the total kinetic energy of

the charged particles that is produced by indirectly ionizing radiation, i.e. neutrons and gamma rays, per unit mass of the irradiated material. The fluence-to-kerma factors will be referred to as "kerma factors". Microscopic kerma factors, i.e. the total kinetic energy released "per material atom" rather than per unit mass, will be the factors used in this work as a matter of convenience.

The heat generation rates will be calculated in terms of predetermined kerma factors for the material composition of the system. Since kerma is concerned only with the energy released at a point rather than the subsequent particle or photon transport and energy deposition, the accuracy of calculating a kerma factor is limited only by the accuracy of the nuclear parameters. For practical purposes, the kerma factor is customarily taken as equal to the energy deposition at the point of neutron interaction[56]. The energy deposition due to the secondary gamma rays produced by neutron radiative capture, inelastic scattering, or other gamma-ray producing reactions will not be included in neutron kerma factors. Separate gamma-ray kerma factors will be used to account for the energy deposition due to the secondary gamma-rays.

Heating by neutrons at any spatial point can be expressed simply as

$$H_n(\vec{r}) = \text{Neutron Heat Generation Rate at } \vec{r} = NC \sum_{g=1}^{IGN} \int_{E^g_{min}}^{E^g_{max}} \sum_j \sigma_j(E)\, E_j(E)\, \phi(E,\vec{r})\, dE \qquad (B\text{-}1)$$

where

σ_j = microscopic cross section of reaction j (cm^2/atom)

E_j = energy deposited by reaction j for a neutron of energy E

$\phi(E,r)$ = neutron flux at r and energy E withing group g

N = nuclide density (atoms/cm^3)

E^g_{min} and E^g_{max} are the lower and upper bounds, respectively for energy group g.

C = conversion factor to convert from the energy units used for E to other convenient units

The sum over g is taken over all neutron energy groups IGN. Equation B-1 can be rewritten as

$$H_n(\vec{r}) = NC \sum_{g=1}^{IGN} \overline{\left(\sum_j \sigma_j E_j\right)}_g \phi_g(\vec{r}) \qquad (B\text{-}2)$$

where

$\phi_g(\vec{r})$ = average neutron flux at r in energy group g (n/cm^2sec)

$K^g_n = \overline{\left(\sum_j \sigma_j E_j\right)}_g$ defined here to be the microscopic kerma factor (or kerma Per unit fluence per atom) for energy group g.

The microscopic kerma factors for the various nuclides of the blanket are determined for a fine energy group structure using either a flat or $\frac{1}{E}$ weighing within a group. The kerma factors for the fine group structure are then weighed with the flux spectrum of a representative fusion shell obtained from a transport calculation to produce kerma factors for the desired group structure intended for use in the blanket design.

The E_j referred to in the above equations is obtained by summing the average initial kinetic energies imported to the struck nuclei and the kinetic energies imparted to the charged particles emitted. The methods used to calculate the energy released by each type of reaction are discussed in ref. (56).

Solomito et al have compiled a neutron kerma library for a limited number of materials. The computer program AVKER[57] evaluates neutron kerma factors for any desired composition that can be made up from elements available in the kerma library for any arbitrary group structure within the energy limits of 19.2 MeV to 0.023 eV.

Since the neutron kerma library is only available for a limited number of materials, the neutron kerma factors for other materials of interest in fusion blanket and magnet shield design need to be calculated.

The gamma-ray kerma factors can be determined from the following expression

$$K_\gamma^g = \overline{E\sigma}_{abs} = \frac{C}{\Delta E_g} \int_{E^g_{min}}^{E^g_{max}} [\sigma_{pp}(E)(E-1.02) + \sigma_{PE}(E)E + \sigma_{c.a.}(E)E]dE \qquad (B-3)$$

where

K_γ^g = the gamma-ray kerma factor for energy group g (ergs/atom)/(gamma/cm^2)

E = gamma-ray energy within group g (MeV)

ΔE_g = energy width of group g

$\sigma_{pp}(E)$ = pair production cross section

$\sigma_{PE}(E)$ = photoelectric cross section

$\sigma_{c.a.}(E)$ = Compton absorption cross section

C = conversion factor = 1.602×10^{-6} ergs/MeV

The energy deposition from pair production is corrected by subtracting 1.02 MeV from the interacting photon energy. This accounts for the fact that while the kinetic energies of the pair produced is deposited at very nearly the point of production, their rest masses are converted to two 0.511 MeV gamma-rays by the annihilation process. The two photons produced in the annihilation process are placed in the appropriate gamma energy group.

Implicit in the use of the above γ-ray energy deposition is the assumption that photoelectric effect, pair production, and Compton scattering are the only processes that contribute to heat deposition, and that all other possible second-order processes are negligible. The code MUG discussed earlier calculates the gamma-ray multigroup cross sections and it can be used for determining gamma ray kerma factors for the same energy group structure which will be used in the gamma-ray transport calculations.

The procedure used in this study is that microscopic neutron and gamma kerma factors are generated by programs AVKER and MUG for 100 neutron energy groups and 21 gamma ray energy groups. ANISN is used next to perform group reduction using a typical fusion blanket flux spectrum. The predetermined microscopic kerma factors are in the units (erg/atom)/(particle/cm^2). The heating rate at point r can be determined by use of the expression

$$\text{Total Heat generated at point } \vec{r} = H(\vec{r}) =$$

$$= C \left[\sum_i N_i \left(\sum_{g=1}^{IGN} K_{ni}^{g} \phi_g(\vec{r}) + \sum_{h=1}^{IGG} K_{\gamma i}^{h} \phi_h(\vec{r}) \right) \right.$$

where

K_{ni}^{g} = kerma factor for neutron group g for nuclide i (ergs/atom)/(n/cm^2)

$\phi_g(\vec{r})$ = neutron flux in group g at r (n/cm^{2}sec)

$K_{\gamma i}^{h}$ = kerma factor for γ group h for nuclide i (ergs/atom)/(gamma/cm^2)

$\phi_h(\vec{r})$ = photon flux in group h (gamman/cm^{2}sec)

N_i = nuclide density (atoms/cm^3)

IGN = number of neutron energy groups

IGG = number of gamma energy group

and C = conversion factor

$H(\vec{r})$ can be calculated then through the ANISN activity option, with the nuclide density input in the mixing table modified with the desired conversion factor C.

The following flow chart shows the various steps for preparing the nuclear data required for computer calculations of this study.

NEUTRON MULTIGROUP X-SECTS.

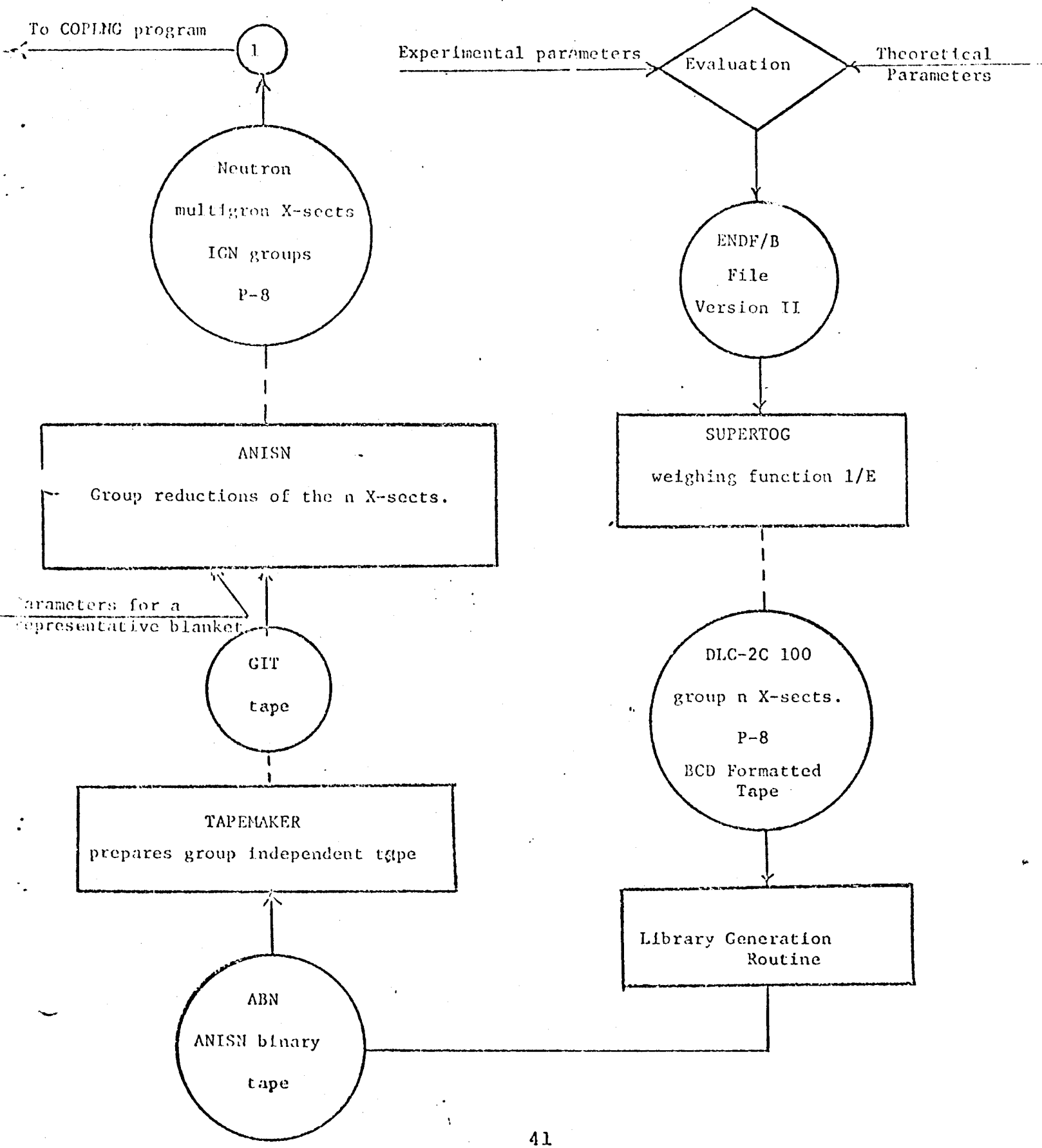

$$KF_\gamma = \frac{1}{\Delta E_g} \int_{E_1}^{E_2} [\sigma_{pp}(E)(E - 1.02) + \sigma_{pe}(E)E + \sigma_{ca}(E)E]dE$$

HPIC

Evaluated Photon Interaction Library for Photoelectric and Pair Production γ-X-sects.

MUG

Calculation of group transfer cross sections using Klein-Nishina formula for Compton scattering. Combines calculated Compton absorption with input photoelectric and pair production X-sects.

γ-ray multigroup X-sects. IGG groups

γ-ray Kerma factors IGG groups

3

To Activity Counter Preparation

2

To Coupling Code

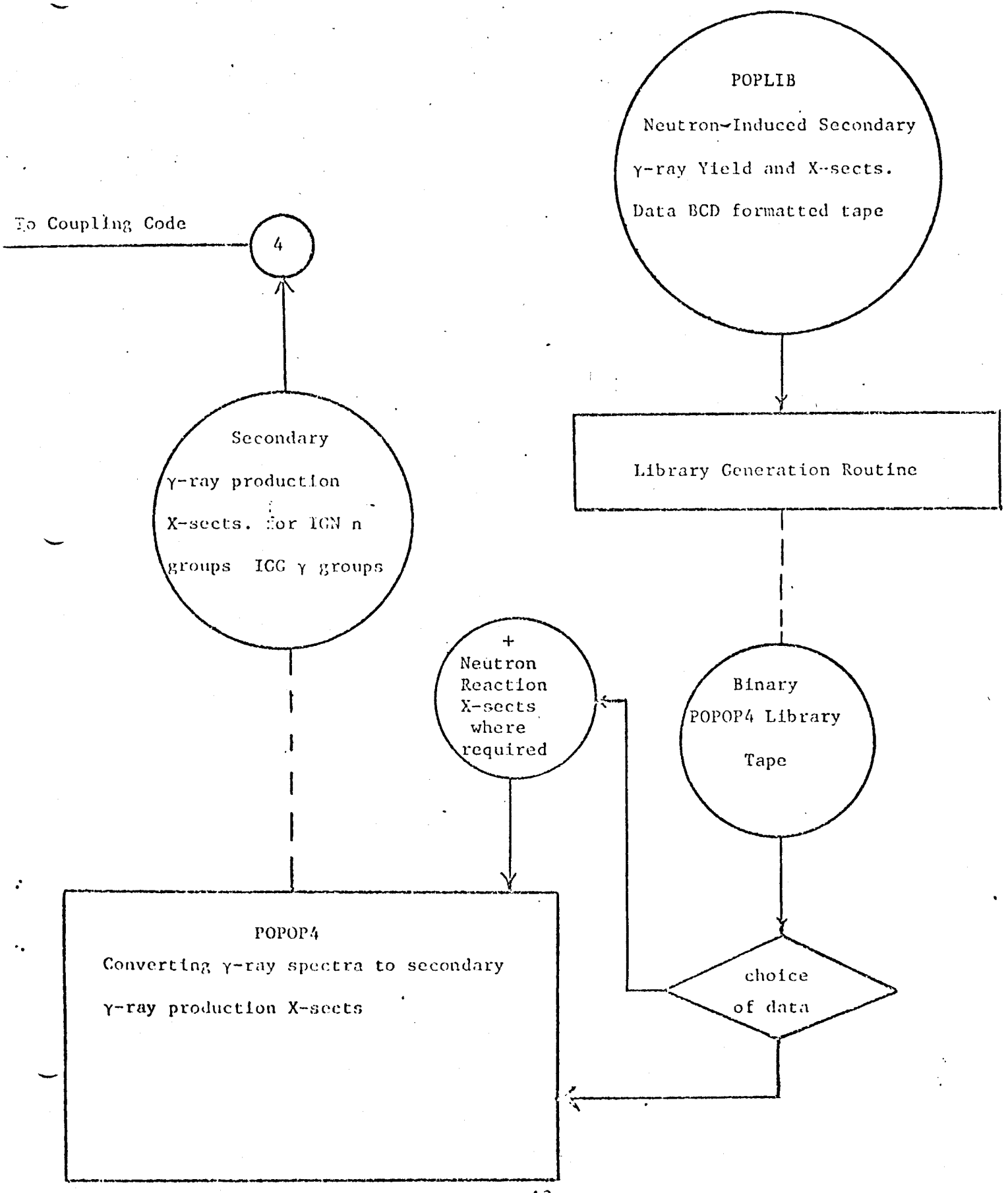
POPLIB
Neutron-Induced Secondary
γ-ray Yield and X-sects.
Data BCD formatted tape
Library Generation Routine
Binary
POPOP4 Library
Tape
choice
of data
+
Neutron
Reaction
X-sects
where
required
Secondary
γ-ray production
X-sects. for IGN n
groups IGG γ groups
4
To Coupling Code
POPOP4
Converting γ-ray spectra to secondary
γ-ray production X-sects

NEUTRON KERMA FACTORS

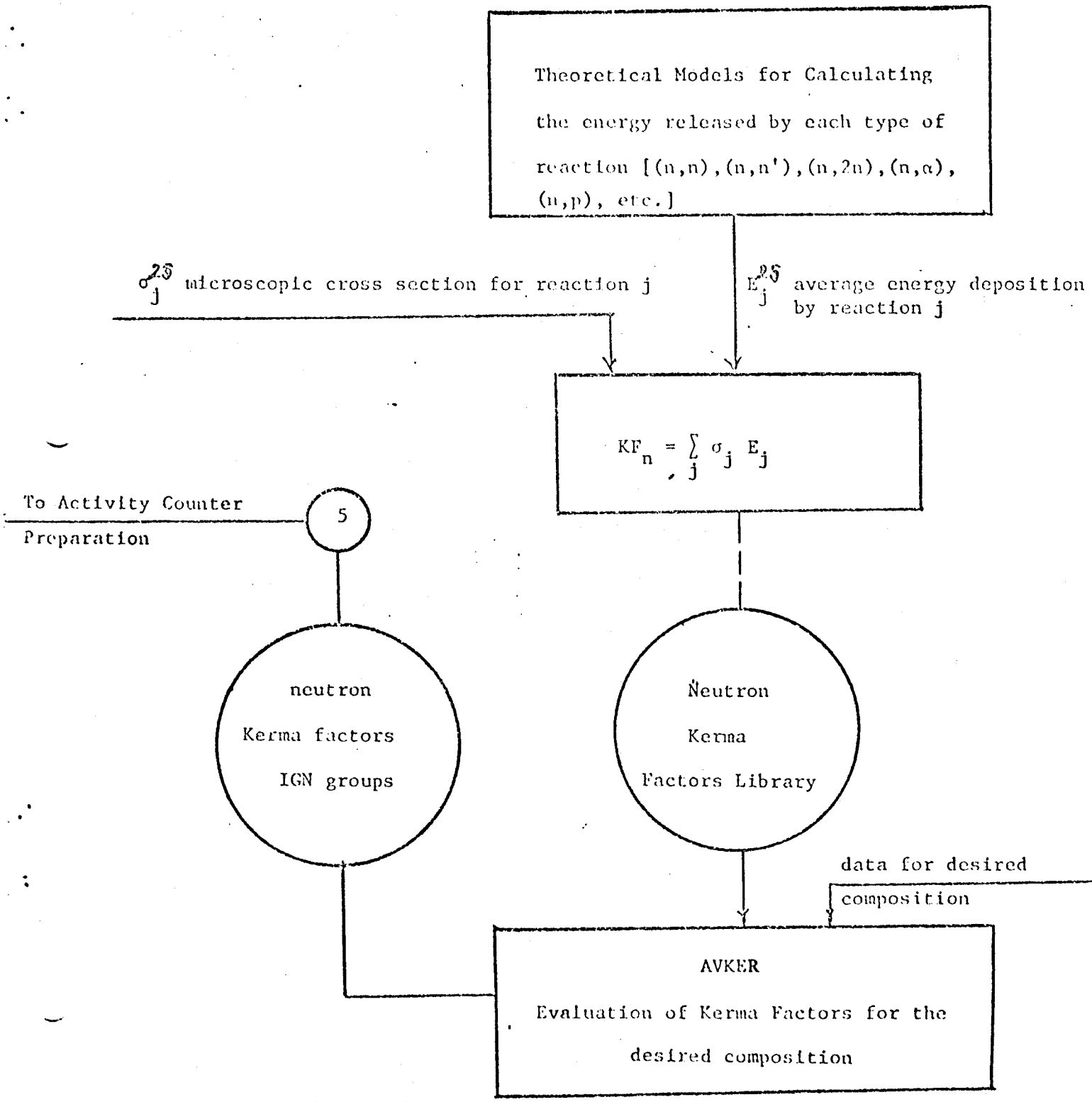

COUPLING AND ANISN CALCULATIONS

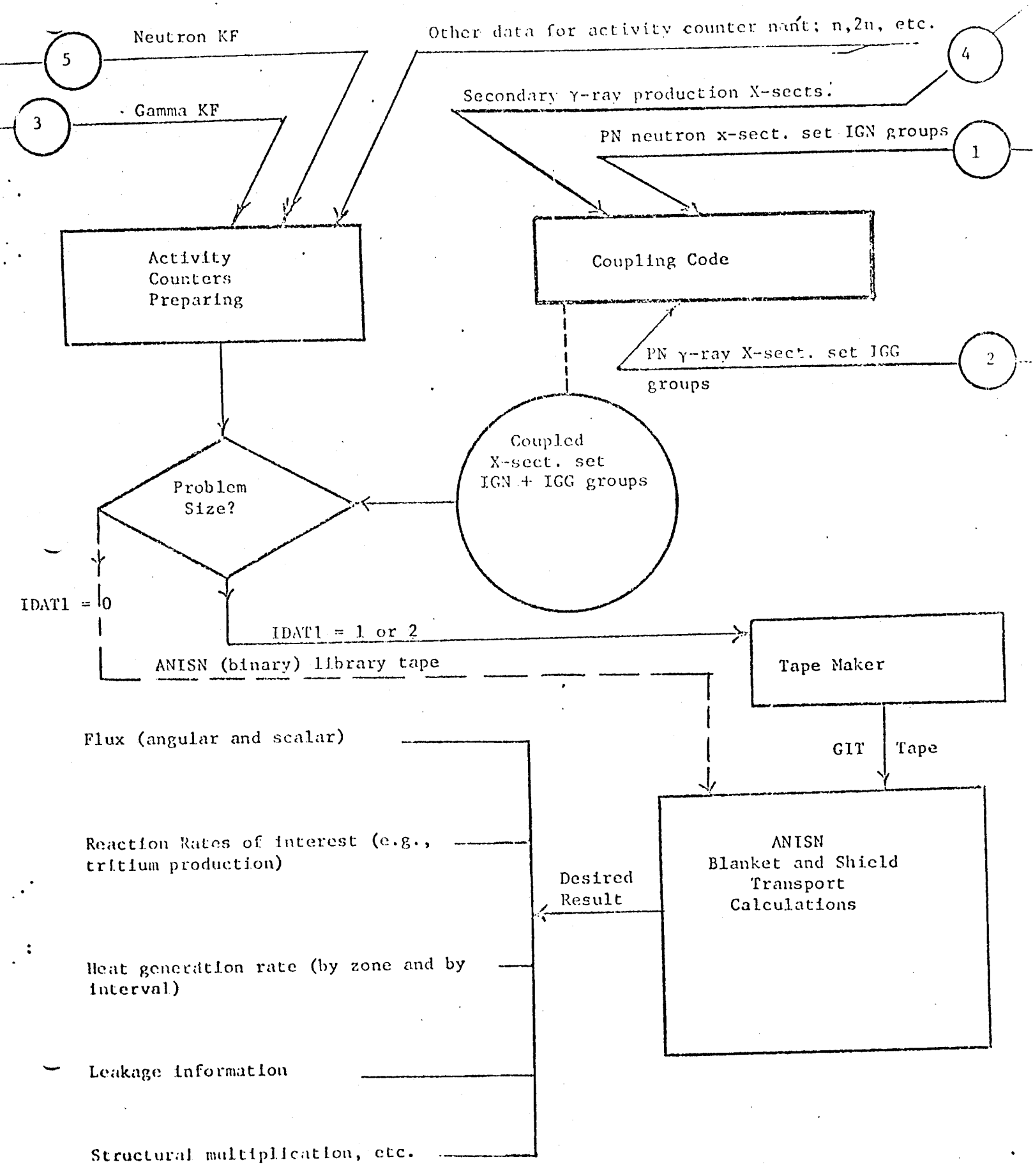

C. The Neutron-Induced Activity of The Blanket and Shield Materials

The blanket and shield materials will be activated by the high neutron flux and the levels of induced radioactivity may be high. For example, Blow[67] has shown that the activity of a segment of the first wall 300 cm in diameter, 0.5 cm thick and 100 cm in length, will be of the order of 17 megacuries at the end of a 20 year irradiation period. The energy release from radioactive decay is also a serious design consideration for loss-of-coolant accidents. D. Dudziak[63] has shown that the afterheat from a 5-GW(th) D-T reactor is at least 30 MW when niobium is used as the structural material. Since radiological hazards, environmental problems and public safety have become of great concern, the induced radioactivity and the afterheat problems form radioactive decay power are important neutronic considerations which enter as constraints on the selection of materials.

In a fusion blanket environment where the neutron energy specturm is wide, the number of possible reactions are large: (n,2n), (n,$\hat{n}$), (n,γ), (n,α), (n,p), etc. Many of the transmutation products are unstable, primarily with respect to β decay and γ-decay of isomeric states. Like the angular flux in transport calculations, investigations of induced radioactivity have an analogous quantity which must be calculated: the reaction products nuclide densities. Unlike fission reactors where one has to calculate the nuclide densities for several hundred fission products, in fusion reactors one has to consider only a few materials which are possible candidates for use in fusion systems. On the other hand, since the number of possible neutron-induced reactions in a fusion blanket environment is

rather large, the number of transmutatin products for each nuclide is large.

One can picutre each nuclide number density as a node[66]. Each node is coupled to one or more nodes by neutron capture, (n,2n), α-decay, beta decay, gamma decay, etc. Figure 4.1 shows some possible transmutations of Ni. The processes can act as sources to Ni. Figure 4.2 indicates the important reactions in niobium activation. These reactions are not all equally important. The dominant reactions vary form one material to another and depend on the flux spectrum. For example, approximately 80% of the activity associated with niobium in a fusion blanket environment is caused by excitation of the first excited state of ^{93}Nb in inelastic scattering. The dominant reactions in the magnet shield are generally not the same as in the blanket.

The balance equation for the nuclide density Ni can be written as:

$$\frac{\partial N_i(\vec{r},t)}{\partial t} = R_i(\vec{r},t) + \sum_j \gamma_j^i N_j - \lambda_i N_i - N_i \int_E \sigma_i(\vec{r},E)\phi(\vec{r},E,t)dE \qquad (1)$$

where

R_i = rate of external addition or removal of nuclide i (introduced for convenience in handling circulated materials)

γ_i^j = the probability per unit time per atom of nuclide j forming nuclide i

λ_i = decay constant of nuclide i

σ_i = microscopic reaction cross section of nuclide i

ϕ = neutron flux

The reaction rates $\int_E \sigma_i(\vec{r},E)\phi(\vec{r},E)dE$ are readily obtainable from the ANISN program computations through the activity option. To simplify the above equation define:

$$A_i(\vec{r}) = \int_E c_i(\vec{r},E)\phi(\vec{r},E)dE$$

$$= \sum_{g=1}^{IGM} \sigma_{ig}(\vec{r})\phi_g(\vec{r}) \qquad (2)$$

where IGM is the number of neutron groups;

$$\beta_i(\vec{r}) = \lambda_i + A_i(\vec{r}) \qquad (3)$$

$A_i(\vec{r})$ is obtained from ANISN calculations at each spatial mesh point, tehn $N_i(\vec{r},t)$ is determined for each spatial point and the total nuclide density $N_i(t)$ is the space integral of $N_i(\vec{r},t)$ over the zones in which nuclide i appears. Therefore, for one spatial point, Eq. (1) can be re-written as

$$\frac{dN_i(t)}{dt} = R_i(t) + \sum \gamma_j^i N_j - \beta_i N_i \qquad (4)$$

$j = 1,2,3,\ldots,J$

$i = 1,2,3,\ldots,I$

These are I coupled sets of 1st order ordinary differential equations and they are a sufficient description of all nuclide number densities.

A difficulty in obtaining a closed form solution arises from the presence of two (or more) nuclides feeding each other. For example Nb^{91m} (see fig. 4.2) decays to the ground state by isomeric transition and the ground state contributes to the isomeric state through the (n,n') reaction. The isomeric states must be generally included because of the relatively long life-time associated with some of these excited states (e.g. Nb^{93M} has a half-life of 13.7 years and in fact, it contributes approximately 80% of the total induced activity in the Niobium chaines as was indicated earlier). Numerical solution of Eq. (4) will be used.

Once $B_i^{,s}$ and $\gamma_j^{i,s}$ and $R_i^{,s}$ at one space point are specified together with the appropriate initial conditions, the set of coupled equations (4) can be solved by numerical integration. With a similar solution for each spatial point the complete solution for the nuclide densities $N_i(r,t)$ is obtained. The induced activity at any time t is simply

$$\sum_{j=1}^{IM} \sum_{i} \lambda_i(\vec{r},t)\Delta V_j(\vec{r})$$

where ΔV_j is the volume of the space interval j and IM is the number of space intervals. After reactor shutdown the set of equations (4) are easy to solve. In fact a closed form solution exists (the nuclides are coupled by radioactive decay only in the absence of a neutron flux). Calculation of afterheat at any time is straight forward once the nuclide densities of radioactive products are calculated and their disintegration energies are known. The afterheat from each material i at time t is $E_i \lambda_i N_i(t)$ where E_i is the energy of emitted particles and gammas.

From the above considerations it is clear that formulation of the activation chains is the first and basic step. In fact, it is the most difficult step because of the lack of data for many reactions and the data uncertainty for many others. A careful quantitative analysis of radionuclide activation must access the contributions from (n,P), (n,α) and other reactions besides (n,γ),(n,2n), (n,n') and (n,3n). The data problems discussed in connection with the transport calculations are more severe in accessment of the magnitude of the induced radioactivity. Also, computing and compiling decay energies is a time-consuming task; but the excellent compilation by T. England[66] will be most helpful in this regard. Mathematical description of the activation chains is straight forward, and calculation of nuclide densities requires an effecient computer program to handle the general set of differential equations showing in Eq. (4).

In summary, the purpose of this part of the study is to compare neutron-induced activity and afterheat for materials which are possible candidates for use in fusion reactor blankets and magnet shields. In addition, the effect of varying the neutron energy specturm, power level, and irradiation time will be examined.

FIGURE 4.1

Some Transmutations of Nuclide N_i (from ref. 66)

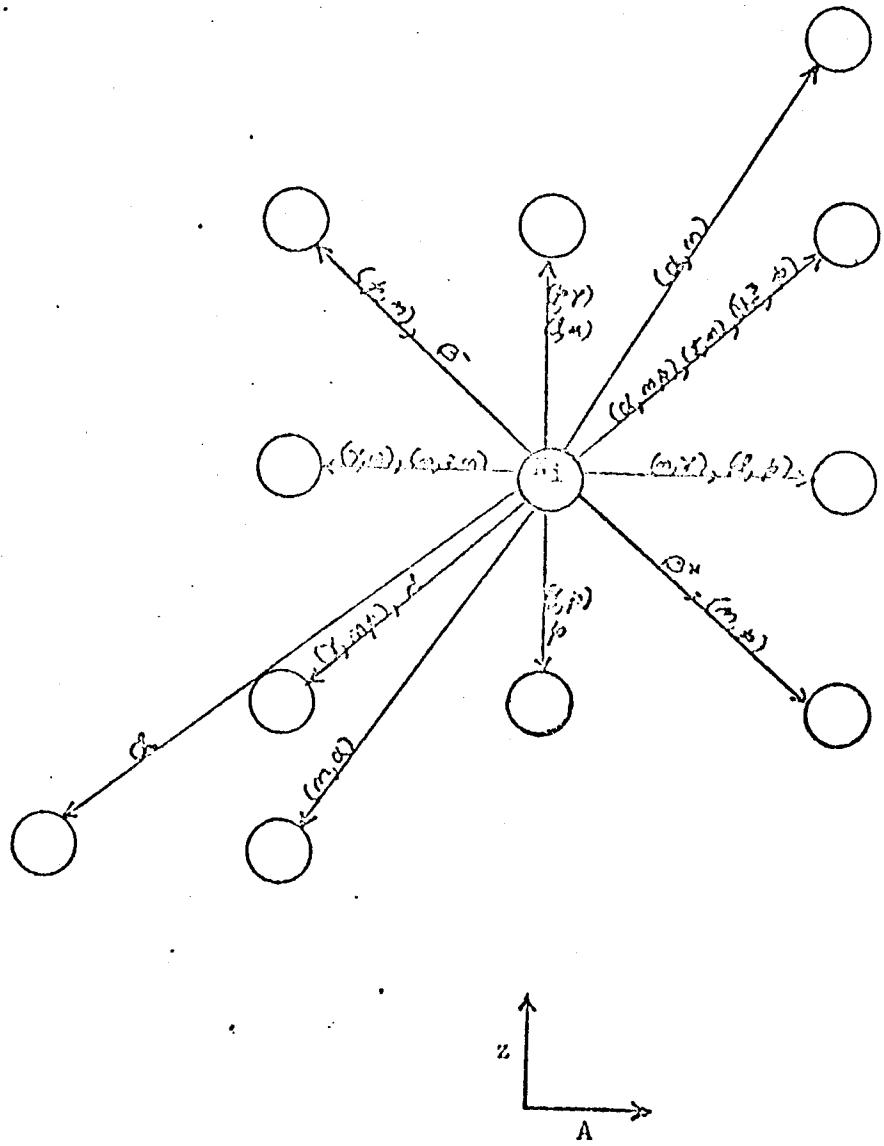

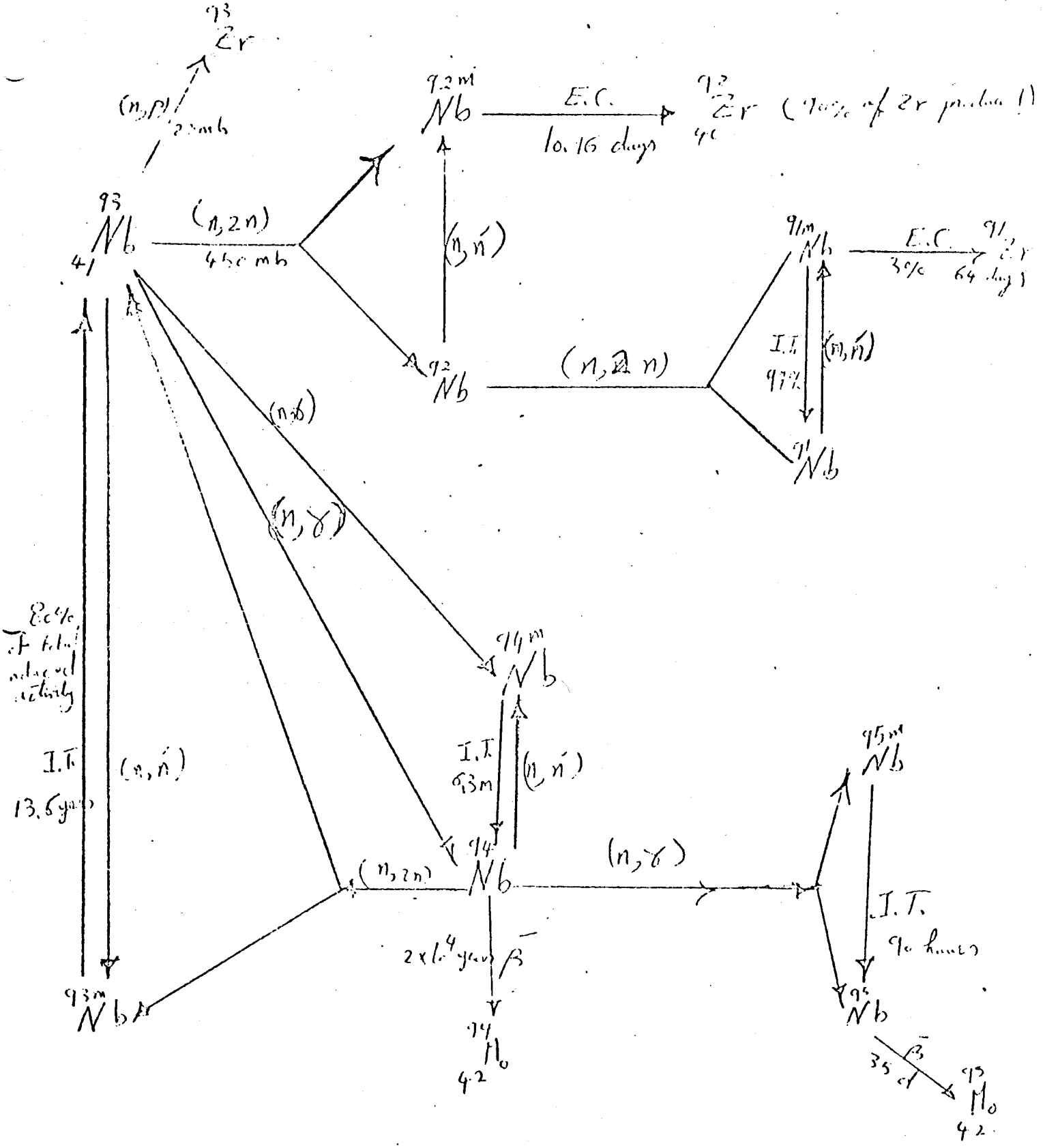

Figure 2) Niobium Activation Chains [26]

Bibliography

(1) L. Spitzer, Jr., D.J. Grove, W.E. Johnson, L. Tonks, and W.G. Westendorp, NYO 5047 (1954)

(2) E.P. Johnson, NYO 7900 (1957)

(3) P.R. Bell and others, ORNL 2457 (1958)

(4) N.C. Christofilos, N.W. Cook, W.B. Myers, C.E. Taylor, and W. Wells TID 7558, Suppl. 1 (1960)

(5) D.J. Rose and M. Clark, Jr., Plasma and Controlled Fusion, 2nd revised printing, M.I.T. Press, Cambridge, Mass. (1965) Chap. 13

(6) A.J. Impink, Jr., Neutron Economy in Fusion Reactor Blanket Assemblies, Technical report No. 434, M.I.T. Research Laboratory of Electronics, Cambridge, Mass. (1965)

(7) W.G. Homeyer, Thermal and Chemical Aspects of the Thermonuclear Blanket Problem, Technical report No. 435, M.I.T. Laboratory of Electronics, Cambridge, Mass. (1965).

(8) L.N. Lontai, Study of a Thermonuclear Reactor Blanket with Fissile Nuclides, Technical Report No. 436, M.I.T. Research Laboratory of Electronics, Cambridge, Mass. (1965).

(9) P.S. Spangler, Fusion Reactor Blanket Experiment, Technical Report 437, M.I.T. Research Laboratory of Electronics, Cambridge, Mass. (1965).

(10) L.M. Petrie, Jr., Gamma-Ray Spectra In Fusion Blanket Mock-Ups, Technical Report 438, M.I.T. Research Laboratory of Electronics, Cambridge, Mass. (1965).

(11) D.J. Rose, "On the Feasibility of Power by Nuclear Fusion," ORNL-TM-2204, Oak Ridge National Laboratory (1968).

(12) D. Steiner, "Neutronic Calculations and Cost Estimates For Fusion Reactor Blanket Assemblies," ORNL-TM-2360 (1968).

(13) A. Fraas, Parameters for a Series of Reference Designs of Thermonuclear Reactors, Appendix III, reference (11).

(14) Proceedings of B.N.E.S. Nuclear Fusion Reactor Conference, Culham (1969).

(15) Blow, S., Crocker, V.S. and Wade, B.O., Neutronics calcualtions for Blanket Assemblies of a fusion reactor, Proceedings of B.N.E.S. Nuclear Fusion Reactor Conference, Culham (1969) Paper 5.5

(16) D. Steiner, Neutronic Behavior of Two Fusion Reactor Blanket Designs, Proceedings of B.N.E.S. Nuclear Fusion Reactor Conference, Chlham (1969) 483.

(17) J.D. Lee, Tritium Breeding and Energy Generation in Liquid Lithium Blankets, Proceedings of B.N.E.S. Nuclear Fusion Conference, Culham (1969) Paper 5.3.

(18) R.W. Werner, Module Approach to Blanket Design-A Vacuum Wall Free Blanket using Heat Pipes, Proceedings of B.N.E.S. Conference, Culham (1969) Paper 6.2.

(19) G.R. Hopkins and G. Melese-d' Hospital, Direct Helium Cooling Cycle for a Fusion Reactor, Proceedings of B.N.E.S. Nuclear Fusion Reactor Conference, Culham (1969) Paper 6.1

(20) R.W. Werner, B. Myers, P.B. Mohr, J.D. Lee, and N.C. Christofilos, Preliminary Design Consideration for an Astron Power Reactor System, Proceedings of B.N.E.S. Nuclear Fusion Reactor Confernece, Culham (1969) Paper 5.2.

(21) E.F. Johnson, Overall Tritium Balances in Fusion Reactors, Proceedings of B.N.E.S. Nuclear Fusion Reactor Conference, Culham (1069) Paper 5.1.

(22) A.P.Fraas, Conceptual Design of a Fusion Power Plant to Meet the Total Energy Requirements of an Urban Complex, Proceedings of B.N.E.S. Nuclear Fusion Reactor Conference, Culham (1969) 1.

(23) D. Steiner, The Nuclear Performance of Fusion Reactor Blankets, Nuclear App. and Tech 9, 83 (1970).

(24) A.P. Fraas and H. Postma, Preliminary Appraisal of the Hazards Problems of a D-T Fusion Reactor Power Plant, ORNL-TM-2822 (Revised) (1970).

(25) A.P. Fraas, Conceptual Design of the Blanket and Shield Region of a Full-Scale Fusion Reactor, ORNL-TM-3096 (1970).

(26) D. Steiner, "The Neutron-Induced Activity andDecay Power of The Niobium Structure of a D-T Fusion Reactor Blanket, ORNL-TM-3094 (1970).

(27) Proceedings of IAEA Fourth Conference on Plasma Physics and Controlled Nuclear Fusion Research, Madison, Wisconsin (June 1971)

(28) H. Borgwaldt, W.H. Kohler, and K.E. Schroeter, Neutronic Thermal Design Aspects of Thermonuclear Fusion Reactor Blankets, Reference (27), Paper CN-28/K-12 (Revised)

(29) D. Steiner, Emergency Cooling and Radioactive Waste-Disposal Requirements for Fusion Reactors, Reference (27), Paper CN-28/K-11

(30) Th. Bohn, and S. Forster, Blanket Cooling Concepts and Heat Conversion Cycles for Controlled Thermonuclear Reactors Reference (27), Paper CN-28/K-13.

(31) A.P. Fraas, A Diffusion Process For Removing Tritium From The Blanket Of A Thermonculear Reactor, ORNL-TM-2358 (1968)

(32) D.K. Trubey and Betty F. Maskewitz, "A Review of the Discret Ordinates S_n Method for Radiation Transport Calculations," ORNL-RSIC-19 (1968).

(33) W.W. Engle, Jr., A User's Manual for ANISN: A One Dimensional Discrete Ordinates Transport Code With Anisotropic Scattering, USAEC Report K-1693 (1967).

(34) M.A. Abdou, A Revised Manual For ANISN-1108 University of Wisconsin Report PLP-429

(35) F.R. Mynatt, A User's Manual for DOT-USAEC Report K-1694 (1967).

(36) K.D. Lathrop, "DTF-IV, a Fortran-IV Program for solving the Multigroup Transport Equation with Anisotropic Scattering", LA-3373, November, 1965

(37) R.Q. Wright, N.M. Greene, J.L. Lucius, and C.W. Craven, Jr., "SUPERTOG: A program to Generate Fine Group Constants and P_n Scattering Matrices from ENDF/B", ORNL-TM-2679 (Sept. 1969)

(38) H.C. Honeck, "ENDF/B - Specifications for an Evaluated Nuclear Data File for Reactor Applications," BNL-50066 (May 1966) Revised 7/1967

(39) DLC-2C, "PSIC Data Library Collection, 99-Group Neutron Cross Section Data based ON ENDF/B" ORNL-TM-3049 (Feb. 1971)

(40) "A Review Of Multigroup Nuclear Cross Section Preparation," ORNL-RSIC-27 (Jan. 1970)

(41) Evans, R.D., The Atomic Nucleas, 1955, Chapter 23, McGraw-Hill Book Co.

(42) Kaplan, I., Nuclear Physics, 1962, Addison-Wesley Publishing Co., Inc.

(43) K.D. Lathrop, GAMLEG-A Fortran Code to Produce Multigroup Cross Sections for Photon Transport Calculations, LA-3267. (1967)

(44) J. H. Renken and K.G. Adams, GAMLEG 69, SC-DC-69-2015 (1969)

(45) M.J. Stanley, "Klein-Nishina Photon Cross Sections (Program GAMMA)," APEX-487, General Electric Company (May 1959)

(46) F. Biggs and Ruth Lighthill, Analytical Approximations for X-ray Cross Sections, SC-RR-66-452 (1966)

(47) F. Biggs and Ruth Lighthill, Analytical Approximations for Total Pair Production Cross Sections, SC-RR-68-619 (1968)

(48) "MUG; Aprogram For generating Multigroup Photon Cross Sections" J.R. Knight, and F.R. Mynatt CTC-17 (Jan. 1970)

(49) "POPOP4: A CODE For Converting Gamma-Ray Spectra To Secondary Gamma-Ray Production Cross Sections" W.E. Ford, III, and D.H. Wallace CTC-12 (May 1969)

(50) H. Goldstein, Fundamental Aspects of Reactor Shielding, Addison-Wesley, Reading, Mass.

(51) W. Heitler, The Quantum Theory of Radiation. Oxford University Press, New York

(52) "POPOP4 Library of Neutron-Induced Secondary Gamma-Ray Yield And Cross Section DATA" CTC-42

(53) L.D. Landau, and E.M. LIFSHITZ Quantum Mechanics, Pergamon Press

(54) George I. Bell, S. Glasstone, Nuclear Reactor Theory, Van Nostrand Reinhold Company, (1970)

(55) J.J. Ritts, M.Solomito, and P.N. Stevens, "Calculation of Neutron Fluence-to-Kerma Factors for the Human Body," Nucl. Applic. and Technology, 7(1), 89-99 (July 1969)

(56) J.J. Ritts, M. Solomito, and D. Steiner, "Kerma Factors AND Secondary Gamma-Ray Sources For Some Elements of Interest in Thermonuclear Blanket Assemblies," ORNL-TM-2564 (June 1970)

(57) "AVKER: A Program for Determining Neutron Kerma Factors for use In Energy Deposition Calculations", M. Solomito, J.J. Ritts, and H.C. Claiborne, ORNL-TM-2558 (April 1969)

(58) GAMII Cross Section Library, these data are available from the Radiation Shielding Information Center (RSIC), Oak Ridge, Tennessee (1971)

(59) Comments On Points Raised In the Account Of Dr. Chernilin's Views (on the possible effect the present status of cross section data could have on tritium breeding ratios and Fusion-fission systems). A letter form W.C. Gough, USAEC, To CTR Technology Group (June 1971)

(60) M.A. Preston, Physics of the nucleus, Addison-Wesley Publishing Co. (1962)

(61) C.M. Lederer, J.M. Hollander and I Perlman, Table of Isotopes, John Wiley and Sons, Inc., New York (1967).

(62) S. Pearlstein, "An Extneded Table of Calculated (n,2n) Cross Sections," Nuclear Data, Section A,3, (1967)

(63) D.J. DUDZIAK, A Technical Note on D-T Fusion Reactor Afterheat, Nuclear Technology 10, 391 (March 1971)

(64) H.C. Claiborne, "Survey of Methods for Calculating GAMMA-RAY Heating", ORNL-RSIC-8 (1965)

(65) Radiation Quantities and Units, compiled by Comission on Radiological Units and Measurements (ICRU), National Bureau of Standard Handbook 84 (ICRU Report 10a) November 14, 1962.

(66) T.R. England, An Investigation of Fission Product Behavior and Decay Heating in Nuclear Reactors, A Ph.D. thesis, Nuclear Engineering Department, University of Wisconsin (1969).

(67) V.S. Crocker, S. Blow, C.J. H. Watson, Nuclear Cross-Section Requirements For Fusion REACTORS, CN-26/987 (CLM-P240) June 1970

(68) Yu.F. Cherrilin and G.B. Yan kov, Nuclear Data For Thermonculear Reactors, CN-261104 (June 1970)

(69) D. Steiner, Neutron Cross-Section REquirements For Fusion Reactor Design, paper presented at the third conference on Neutron Cross Sections and Technology at the Univ. of Tennessee (March 1971)

(70) L.I. Schiff, Quantum Mechanics, Third Edition (1968) McGraw-Hill Book Co.

(71) H. Green span; C.N. Kelber, D. Okrent, Computing Methods in Reactor Physics, Gordon and Breach Science Publishers, (1968). (Chapter 3 about the Discrete ordinates method is written by B.G. Carlson, and K.D. Lathrop).

(72) C.E. Lee, The Discrete S_n Approximation To Transport Theory, LA-2595 (march 1962).

(73) K.D. Lathrop and B.G. Carlson, "Discrete Ordinate Angular Quadrature of the Neutron Transport Equation", LA-3185 (Feb. 1965).

(74) A. Weinberg and E. Wigner, The Physical Theory Of Neutron Chain Reactors, The University of Chicago Press (1958).